Proceedings of the ASME-JSME-KSME 2019
8th Joint Fluids Engineering Conference
AJKFluids2019
July 28-August 1, 2019, San Francisco, CA, USA

AJKFluids2019-5041

NUMERICAL STUDY ON UNSTEADY WAKE CHARACTERISTICS OF AN URBAN MAGLEV TRAIN

Zhenxu SUN
Key Laboratory for Mechanics in Fluid Solid Coupling Systems, Institute of Mechanics, Chinese Academy of Sciences
Beijing, China

Yongfang YAO
Key Laboratory for Mechanics in Fluid Solid Coupling Systems, Institute of Mechanics, Chinese Academy of Sciences

Fanbing KONG
CRRC Tangshan Co., Ltd
Tangshan, Hebei, China

Guowei YANG
Key Laboratory for Mechanics in Fluid Solid Coupling Systems, Institute of Mechanics, Chinese Academy of Sciences
Beijing, China

ABSTRACT

As the running speed increases, the aerodynamic loads become dominant for high-speed ground vehicles. Meanwhile, the aerodynamic lift of the trailing car becomes crucial at higher speed, which may lead to security and comfort problems. Flow field details are the root to the aerodynamic loads. Study on the wake characteristics of the train could shed light to learn the mechanism of their aerodynamic loads and know how to improve their aerodynamic performance. In the present paper, the urban maglev train with a design speed of 200 km/h is mainly focused on. Numerical investigation is adopted for current study. The Improved Delayed Detached Eddy Simulation (IDDES) numerical approach is utilized to count for unsteady flow details. To characterize the vortex structures, the iso-surface of Q for urban maglev train is obtained and compared. Due to the existence of guide way, the streamline of maglev trains is much more influenced by the guide way. The ground effect for maglev trains is more obvious. The streamlined shape is quite essential to the flow phenomena, and as a result, the vortex structures for urban maglev trains are also different. Guide way could lead to more vortices, which is common for maglev trains. However, lateral vortex could be observed for urban maglev trains, which is unique and is a result of the flat shape of the trailing nose. Meanwhile, the slipstream in the wake of the train is also compared. The streamlined shape of urban maglev trains is the bluntest, which induces the relatively biggest train wind. Based on the above analysis, the unsteady characteristics of flow field for urban maglev train are obtained and the main vortex structures are characterized. Based on the unsteady analysis of flow field, the relationships between aerodynamic loads of the trailing car and different kinds of trailing vortices are obtained. Current study could shed light on the understanding of mechanism of aerodynamic performance of a train and how to design the streamlined shape for trains with certain operational speed.

1 INTRODUCTION

Urban Magnetic Levitation (Maglev) Trains, usually operating at speeds from 100 km/h to 200 km/h, become an important transportation tool in big cities and play a more and more crucial role nowadays. It experiences a booming development for urban maglev trains in China in last decade and two representative lines could be found, which are the urban maglev line in Changsha and the S1 line in Beijing. The former line, starting from Changsha South Station to Huanghua International Airport, was designed with a maximum operation speed of 100 km/h. The latter was designed in 2018 with a maximum running speed of 120 km/h. Moreover, according to the 13th Five-Year Project in China, designing an urban maglev train with a running speed of 200 km/h is a key task, which imposes a challenge to its aerodynamic design. A conceptional design of the train is shown in Figure 1. In general, along with the increase of operation speed of urban maglev trains, the requirement for their aerodynamic performance becomes stringent. Due to the strong coupling of the train body and the guide way, which is also a distinctive difference from high speed

trains, aerodynamic study on urban maglev trains tends to be more challenging.

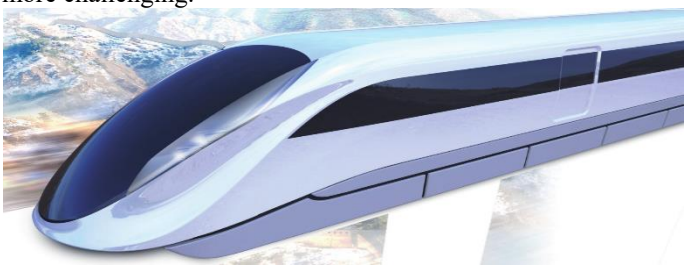

Figure 1 Conceptional design of an urban maglev train

Similar to high speed trains, flow around maglev trains is also highly turbulent with severe unsteady characteristics [1]. For maglev trains, two main regions should be deeply focused on: the wake zone and the clearance zone between the guideway and the train body. When trains run at a certain speed, strong helical vortices could be found in the wake zone. They generate in the boundary layer of the train, get separated and detached from the trailing streamline, and finally, exhibit serious transient characteristics. Meanwhile, due to the disturbance of the bottom surface of the train and the guideway, flow in the clearance zone is also highly unsteady, which could result in unsteady pressure fluctuation and do harm to the structure of the train body.

For the research on train aerodynamics in the last few decades, no matter maglev trains or high speed trains, most of them are simplified to steady problems. However, according to the above analysis and recent studies [1-4], it is very necessary to study unsteady aerodynamic characteristics of trains, most of which mainly focus on high speed trains. From the view of abroad, Baker [1, 4-6] carried out thorough study and obtained fruitful results on aerodynamic performance of simplified trains running in the open air or in cross wind conditions, no matter time-averaged or transient characteristics, with use of full scale experiments, reduced scales experiments and numerical simulations. Taking the unsteady aerodynamic loads from reduced model experiments and numerical simulations as input, Baker [7] also carried out a research on dynamic response of trains under excitation from aerodynamic loads. Hemida and Krajnovic [2, 8-11] introduced Large-eddy Simulation method (LES) into the study of trains aerodynamics for the first time, and comparatively validated the results with experiments. Simplified train models were adopted in their study due to a compromise with numerical cost. Their results revealed the influence of detached helical vortices on the unsteady aerodynamic loads on the trailing car is serious. Meanwhile, dominant frequencies of the aerodynamic loads and the transverse movement of the train body are really close to each other, which could further deteriorate the unwanted transverse movement of the train. These results were all validated by the experimental data. Moreover, the influence of different yaw angles and lengths of streamlined shape on unsteady cross wind effect was also investigated by them. More recently, unsteady characteristics of the flow around a freight train in the cross wind with a yaw angle of 90° were studied by Hemida and Baker [12] with use of LES method, and the influence of moving ground on the lift and lateral forces was under investigation as well. Flow characteristics of an ICE train model on a 6m-height embankment were researched by Diedrichs [13] numerically and experimentally. Results revealed that aerodynamic performance of the train turned out be worse when running in the leeward of the embankment than in the windward side. Besides, study on aerodynamic loads of a simplified train model in cross wind conditions with different yaw angles was also performed by Diedrichs [14]. Khier et ac [15] carried out a study on the development of flow field and vortex structures around a simplified train model under different cross wind conditions. Results showed that there is a close relationship between yaw angles and vortex structures. Many literatures could be referred to in China on the study of unsteady characteristics, most of which are also about high speed trains or freight trains. Taking different types of freight trains and passenger trains in cross wind conditions into consideration, transient numerical simulations were performed by Zhou [16-18], to compare the influence of running velocity, cross wind velocity and height of embankment on aerodynamic loads. The Lattice-Boltzmann method was adopted by Wang et ac [19] to study the unsteady aerodynamic loads and flow structures for a real train model running in the open air, in cross wind conditions and in the tunnel. Ma et al [20] investigated on the transient aerodynamic loads of a two-dimensional train model with use of LES method. Based on the results from Jing Ma, a three-dimensional model was focused on by Yang [3] to get the dominant frequency of the transient loads, which could shed light on the safety and stability analysis for trains running in cross wind conditions.

Generally speaking, most of the previous study on unsteady aerodynamic characteristics of trains focus on time-variant aerodynamic loads of different carriages, including the fluctuation amplitude and dominant frequencies, which could provide a series of accurate and comprehensive data for the following safety and stability analysis. However, few study could be found to qualitatively and quantitatively investigate the transient characteristics in light of turbulent structures, which is urgently needed for practical application. Moreover, current aerodynamic study on maglev trains tends to focus on time-averaged performance, indicating unsteady study on maglev trains should be strongly pushed forward. In the present paper, the IDDES method is employed for numerical analysis, and the urban maglev train with a running speed of 200 km/h is chosen under investigation. Rather than the clearance zone, the wake zone of the maglev train is focused on in the present paper. Taking into consideration those turbulent variables, such as Q criterion, turbulence kinetic energy and slipstream velocity, we could analyze the unsteady wake characteristics of the maglev train qualitatively and quantitatively, which could aid in the in-depth study of shape optimization and aerodynamic performance assessment.

2 NUMERICAL ALGORITHMS AND VALIDATION

2.1 IMPROVED DELAYED DETACHED EDDY SIMULATION

IDDES is a hybrid RANS-LES model which provides a more flexible and convenient scale-resolving simulation model for flows with a high Reynolds number [21]. Compared to the standard DES model, it has inbuilt methods to prevent against grid-induced separation. Moreover, the model is designed to allow the LES simulation of wall boundary layers at much higher Reynolds number than the standard LES model. Therefore, IDDES is chosen for numerical simulation. The turbulence model used with IDDES is the SST K-W two-equation model.

The commercial software package STAR-CCM+ is used in this study, and the temporal terms for all of the IDDES simulations were discretized by using a second-order backward implicit scheme. The diffusive and sub-grid fluxes were discretized using a Hybrid Guass-LSQ scheme [22]. The convective term was discretized using a second-order hybrid-BCD scheme [23].

2.2 NUMERICAL VALIDATION

In this section, numerical validation is performed by comparisons with experimental results and numerical results (with URANS and IDDES results included). The experiments were carried out by Storms BL in the NASA Ames wind tunnel with the section of 7×10 feet. The experimental model is shown in Figure 2, where the length of the model is 2.476m, the height H is 0.451 m and the width W is 0.3238 m. The velocity of incoming flow is 90.26 m/s. The Reynolds number based the width and the incoming flow is 2×10^6. Due to relatively small size of the model, the densified zone is reduced reasonably when meshing the computational domain, in which the smallest size of the grids is 0.022H. The total grid amount is about 8.5 million.

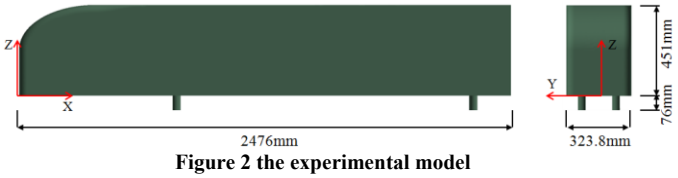

Figure 2 the experimental model

Figure 3(a) shows the experimental setup of the wind tunnel. When performing numerical simulation, the computational domain is chosen as the same with the experiment, as shown in Figure 3(b).

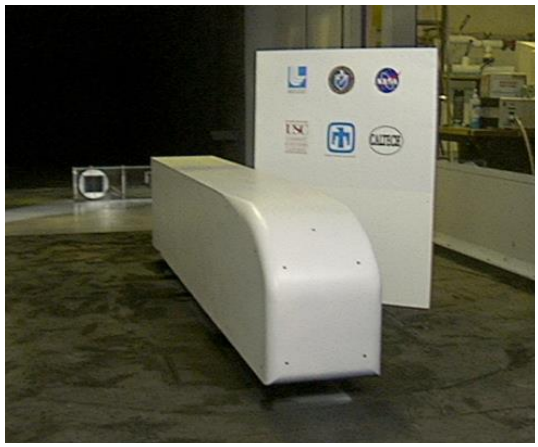

(a)

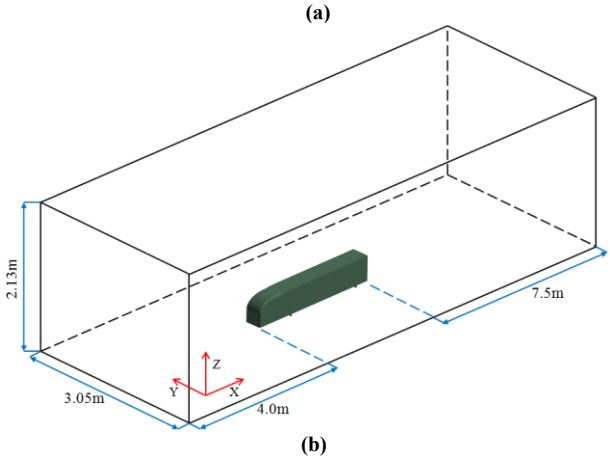

(b)

Figure 3 Experimental and numerical setup of the model: (a) experimental setup; (b) computational domain

Figure 4(a) and Figure 4(b) show the instantaneous vorticity contour in the longitudinal section for URANS and IDDES respectively. Flow structures in the upstream of the model keep nearly the same. However, smaller vortices could be observed in the wake of the model for IDDES while less flow details could be found for URANS method.

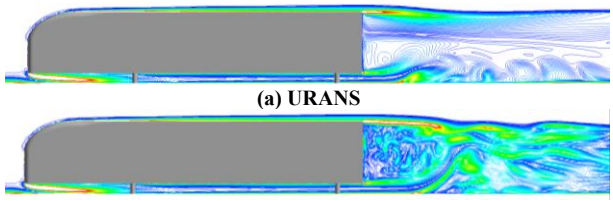

(a) URANS

(b) IDDES

Figure 4 Instantaneous vorticity contour in the longitudinal section for URANS and IDDES: (a)URANS (b)IDDES

The comparison of pressure distribution along the model surface will be performed in three aspects, as show in Figure 5, where the x-coordinate is normalized by the width W and the y-coordinate is normalized by $0.5\rho v^2$.

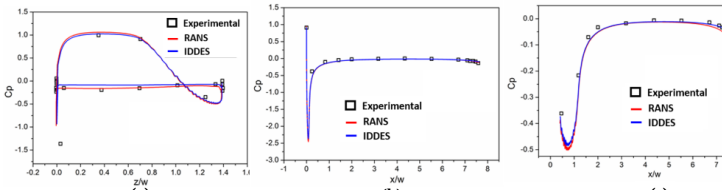

Figure 5 Comparison of pressure distribution along the model surface: (a) height direction; (b) streamwise pressure distribution along the horizontal section; (c) streamwise pressure distribution along longitudinal section

Figure 5(a) shows the comparison of the three methods along the height direction in the longitudinal section, in which the upper part is the pressure distribution along the frontal profile while the lower part is that along the rear profile. It could be seen that both numerical methods get similar results in the frontal profile while differ in the rear. Pressure distribution in the rear profile appears more uniform for the IDDES compared to URANS. Figure 5(b) shows the streamwise pressure distribution along the horizontal section with a height of 0.303m. The flow gets stagnated in the frontal of the model, where pressure coefficient equals nearly to 1. After passing by the stagnation zone, the flow accelerates and its velocity reaches maximum at the lateral sides of the head. In the rear of the model, the pressure decreases again due to the flow separation. Two numerical results both agree well with the experimental results along the section profile. Figure 5(c) shows the streamwise pressure distribution along the upper profile of the longitudinal section. As shown in Figure 5(c), when airflow passes the head of the model, pressure drops dramatically due to the curvature change of the model. After that, the pressure of the flow keeps stable until the flow reach the rear of the model, where flow gets separated and a strong shear layer generates, resulting in further pressure drop. Comparing numerical results with the experimental results, it can be seen that all the results agree well in the upstream of the model while numerical results get diverged from each other in the rear part, of which the IDDES approach gives the better prediction results.

Since the unsteady characteristics in the wake zone of the train are the primary focus in the present study, IDDES will be adopted as the numerical approach on the base of previous validation.

3 COMPUTATIONAL MODELS, MESH AND CONDITIONS

The computational model originates from the conceptional design from the 13th Five-Year project, which is comprised of one leading car and one trailing car. The connection part between two cars are enclosed smoothly with adjacent surfaces, just as shown in Figure 6. The train is running above the guideway with a clearance of 10 mm.

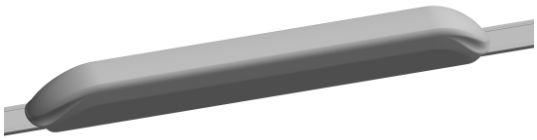

Figure 6 The maglev train model

The hybrid Cartesian/prism grids are adopted and 8 layers of prism grids are generated with an increasing ratio of 1.2 and a total length of 30mm, which keeps the value of y+ of the first layer near the train surface around 1. The grids on the longitudinal and horizontal sections of the domain are shown in Figure 7:

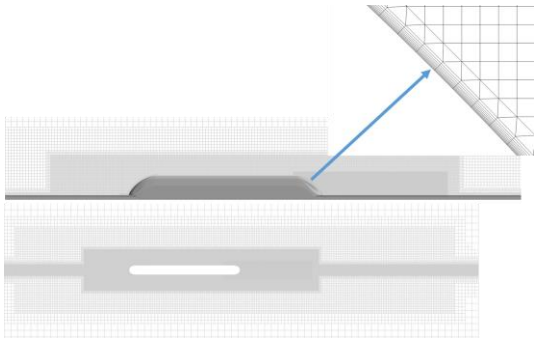

Figure 7 The grids on the longitudinal and horizontal sections of the domain

The computational domain is shown in Figure 8. Taking the height of the train H as the characteristic length, the distance from the inlet boundary to the leading nose is about 14H, while the distance from the trailing nose to the outlet boundary is 38H. The width and height of the domain are 30H and 22H, respectively.

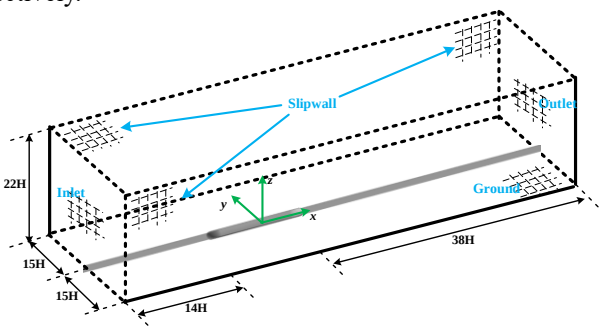

Figure 8 Computational domain

The flow velocity is 200km/h, and the Mach number is 0.16, indicating the flow around the train could be assumed incompressible. Consequently, an incompressible solver is adopted for present study. As for the boundary conditions, a uniform incoming velocity of 200 km/h is prescribed on the incoming boundary, while a zero-pressure condition is imposed on the outlet boundary. A slip wall condition is set to lateral and upper boundaries. For the ground and the guideway, due to their

relative movement with the train, a moving wall condition with the speed of 200 km/h is prescribed on these two boundaries. For the unsteady simulation, the time-step is set as $\Delta t = 1 \times 10^{-4} s$.

4 RESULTS AND DISCUSSIONS

In order to characterize the unsteady wake flow details for urban maglev train, several physical variables are utilized in the present paper, which are Q criterion, turbulence kinetic energy (TKE) and slipstream velocity (TW).

Q criterion, which is the second invariant of the velocity gradient, is defined as below:

$$Q = \frac{1}{2}[(u_{i,i})^2 - u_{i,j}u_{j,i}]$$

Q criterion represents the local balance between the shear strain rate and vorticity magnitude. The region of positive Q implies that the rotation tensor dominates over the rate of strain tensor.

TKE is the mean kinetic energy per unit mass associated with eddies in turbulent flow. Physically, it is characterized by root-mean-square velocity fluctuations. It could be quantified by the mean of turbulence normal stresses:

$$k = \frac{1}{2}[\overline{(u')^2} + \overline{(v')^2} + \overline{(w')^2}]$$

TKE is an intuitive variable to represent the turbulence level of local flow, which is dissipated by viscous forces at the Kolmogorov scale.

Slipstream is created as air is dragged by the movement of a train due to fluid viscosity, the study of which could be important for understanding possible interactions with objects and people. In numerical simulation, train models are usually assumed stationary while the air is passing by with a speed equal to the train velocity. Slipstream velocity could be defined under such condition:

$$TW = \sqrt[2]{(u - u_{train})^2 + (v)^2}$$

The vertical movement of flow is not considered for slipstream velocity.

Taking H as the characteristic length and train velocity V as the characteristic velocity, all the three variables could be transformed into dimensionless forms for analysis.

4.1 COMPARISON OF Q CRITERION

The iso-surfaces of Q criterion at values of 3.97 and 19.84 in the wake of the train model are shown in Figure 9:

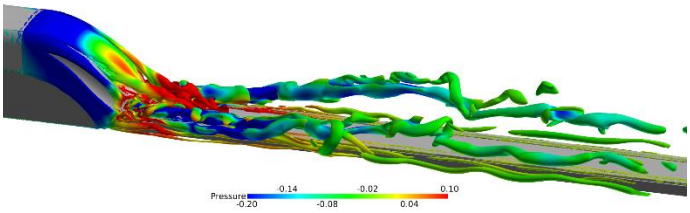

(a)

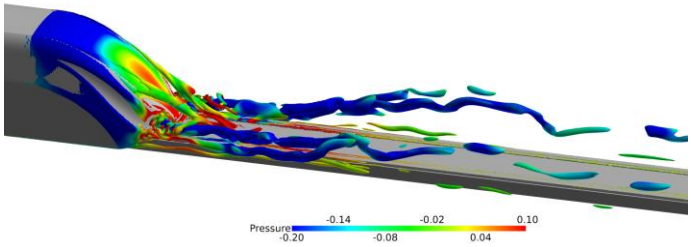

(b)

Figure 9 The iso-surfaces of Q criterion in the wake of the train model: (a) Q of 3.97; (b) Q of 19.84

In order to adapt to the existence of guideways, the nose tip of the train has to be wide and flat. Since the design speed of the urban maglev train is relatively small, the head shapes of the train are usually blunter than that of high speed trains [24], which could result in completely different vortex structures. As seen in Figure 9(a), vortex structures of the urban maglev train originate from the strong interaction between the wide nose and the guideway, and narrow clearance leads to finer vortex structures. Four major helical vortices could still be observed in the wake. For the two vortices on each side, one originates from the nose tip while the other one originates from the bottom of the head. These two vortices tend to curl around each other during the propagation and finally evolve into a bigger vortex. Vortices propagate upwards in the wake zone. This is a key feature for urban maglev trains with a blunt head shape. The height of the wake zone is taller than that of high speed trains, and the vortex structures in the wake are less influenced by the flow with higher speed outside the wake zone. Consequently, the helical vortices tend to grow higher. Since the length of the head is relatively short, another two big vortices detach from the shoulders of the train, which is a result of strong shear stress there. As shown in Figure 9(b), when Q grows higher, only those strong vortices could be reserved while those weaker will disappear. It can be seen that the two vortices in the shoulder and the four vortices in the wake still exist, which contribute to the main characteristics of the wake of urban maglev trains. Viewing from a bigger wake zone, it could be seen that the unsteady turbulent zone is rather big for urban maglev trains due to the upward propagation of strong vortices below.

Figure 10 shows the Q contour at three different cross-sections ranging from H, 2H and 3H in the wake, which could exhibit the decaying of turbulence in the wake.

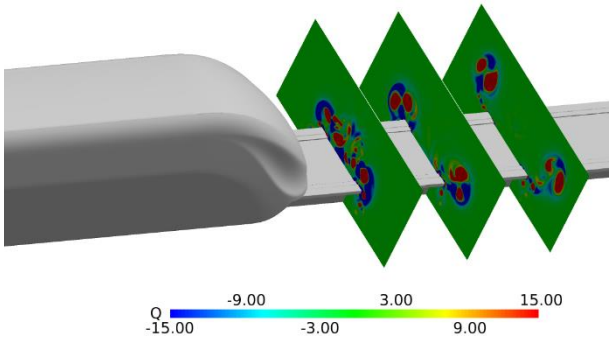

Figure 10 Q contour at three different cross-sections

It could be seen that the guideway is a main source to provide energy for the trailing vortices. Major vortices distribute along the shoulder of the guideway. When it is closer to the trailing nose, cross-section of H for instance, strong vortices could also be observed in the middle of the guideway, which is mainly influenced by flow around the clearance between the nose tip and the guideway. When propagating downstream, the vortices tend to gather on the shoulders of the guideway and grow bigger and bigger.

To investigate on the evolution of trailing vortices in the vertical direction, Q contour on four horizontal sections with heights of 1/8H, 1/6H, 1/3H and 1/2H is show in Figure 11:

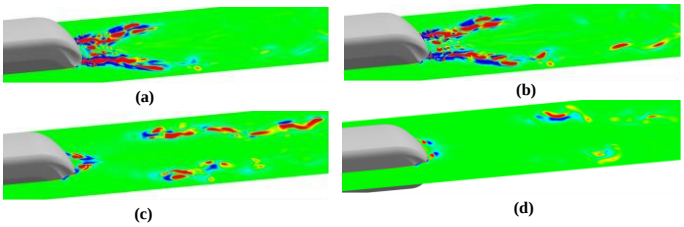

Figure 11 Q contour on four horizontal sections: (a) 1/8H; (b)1/6H; (c)1/3H; (4) 1/2H

At the section of 1/8H, the vortices are concentrated in the near wake zone. They detach from the lateral sides of nose tip and propagate outward. The influence of these vortices are rather limited at this height. Focusing on the section of 1/6H, it could be seen that the strength of vortices is weaker than that on the section of 1/8H. Among the four sections, the section of 1/8H owns the strongest vortices, indicating that interaction between the nose and the guideway is the main source for trailing vortices. At the section of 1/3H, the vortices just behind the nose become smaller and weaker. Meanwhile, due to the upward propagation of trailing vortices below, strong vortices could also be seen at the downstream at this section. For the section of 1/2H, the main vortices are those behind the nose, which is a result of shear layer stress. The influence of upward propagation effect could still be observed in the downstream. Generally speaking, considering the blunt streamlined shape of urban maglev trains, strong influence could be seen in vertical direction, which couldn't be a problem for trains with better streamlined shapes.

4.2 COMPARISON OF TURBULENCE KINETIC ENERGY

The evolution of trailing vortices could also be studied from the view of TKE. TKE generates rapidly near the nose and dissipates quickly in the downstream, which is an evidence of the strong intensity and strong dissipation of local shear layer. Figure 12 shows the TKE contour on the cross-sections of H, 2H and 3H from the trailing nose:

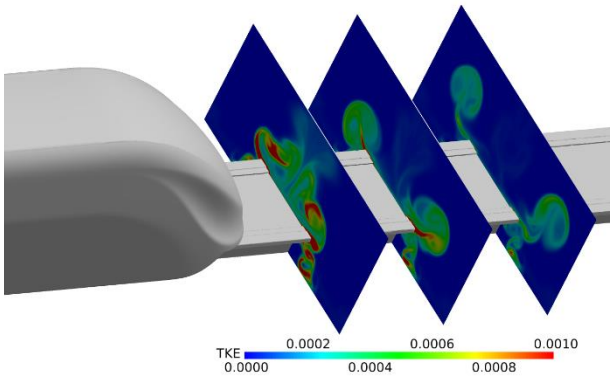

Figure 12 TKE contour on the cross-sections

It could be seen that strong turbulence will be generated by the interaction between the nose and the guideway. Moreover, the shear induced by the flow when passing by the guideway provides the input for turbulence structures, and maintains the strength of these vortices to a certain extent, which is the same conclusion with Q contour analysis.

Figure 13 shows the streamwise distributions of TKE at different heights. Two heights, 1/8H and 1/6H, are chosen for analysis. At each height, different spanwise distances from the centerline of the train are analyzed. Y=0 is the centerline of the train, and the other three lines from the centerline are 0.25H, 0.5H and 0.8H, respectively. For each line, it starts from the very tip of the nose as indicated x=0 in the figures below.

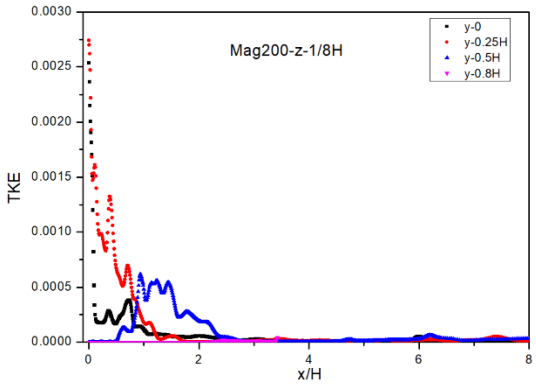

(a)

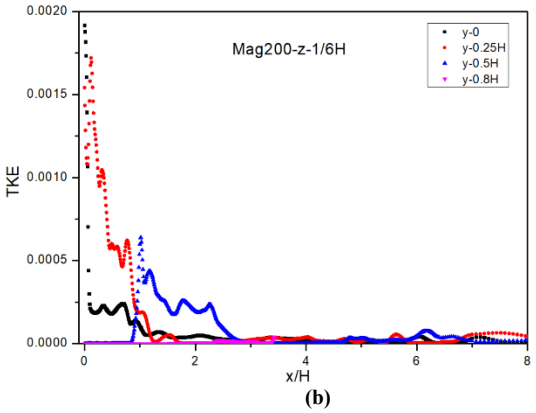

Figure 13 Streamwise distributions of TKE at different heights: (a) 1/8H; (b)1/6H

At the height of 1/8H, main turbulence zone locates in the zone within lines y=±0.25H. TKE rises at the very beginning and then drops after a certain distance at line y=0.5H, which is a result of spanwise movement of turbulence structures along with the corresponding energy transfer. At the height of 1/6H, the tendencies of the lines are more or less the same with that of the height of 1/8H, except that the magnitude is a little lower, indicating the high turbulence zone concentrates at where the nose and the guideway interacts strongly.

4.3 COMPARISON OF SLIPSTREAM IN THE WAKE

It is widely accepted that slipstreams are key unsteady characteristics of trains, which could be a possible threat to the safety of passengers on the platform and railway workers. In this section, the ensemble averaged slipstream velocity is analyzed at different places. Figure 14 shows the streamwise distribution of slipstream velocity at the height of 1/2H. Two distances, 0.5H and 0.8H, are analyzed in current study.

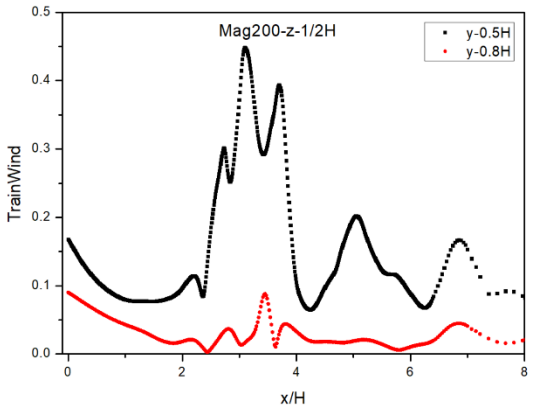

Figure 14 Streamwise distribution of slipstream velocity at the height of 1/2H

It could be observed that the peak of slipstream appears at places from 3H to 4H, which is a direct consequence of upward movement of trailing vortices. These vortices induce strong flow disturbance in this region. Moreover, due to the rather blunt streamlined shape, the magnitude of the slipstream velocity is relatively larger than high speed trains.

5 CONCLUSIONS

Based on IDDES method, unsteady numerical simulation was carried out, from the view of Q criterion, turbulence kinetic energy and slipstream, to qualitatively and quantitatively investigate on the wake characteristics of an urban maglev train with a running speed of 200 km/h. The main conclusions are as follows:

1) The vortices from the bottom and the shoulders are the main characteristics of the studied urban maglev train, and are the main turbulent structures in the wake zone. Generally speaking, unsteady turbulent zone is rather big for urban maglev trains due to the upward propagation of strong vortices below.

2) The guideway is a main source to provide energy for the trailing vortices. Major vortices distribute along the shoulder of the guideway. When it is closer to the trailing nose, strong vortices could also be observed in the middle of the guideway. When propagating downstream, the vortices tend to gather on the shoulders of the guideway and grow bigger and bigger.

3) Strong turbulence will be generated by the interaction between the nose and the guideway. Moreover, the shear induced by the flow when passing by the guideway provides the input for turbulence structures, and maintains the strength of these vortices to a certain extent.

4) Turbulence kinetic energy varies at different locates, Due to movement of vortex structures, energy transfer takes place correspondingly, resulting in the differences of turbulence kinetic energy.

5) the peak of slipstream appears at places from 3H to 4H, which is a direct consequence of upward movement of trailing vortices. Moreover, due to the rather blunt streamlined shape, the magnitude of the slipstream velocity is relatively larger than high speed trains.

ACKNOWLEDGMENTS

This work was supported by Advanced Rail Transportation Special Plan in National Key Research and Development Project under 2016YFB1200601-B13. And Computing Facility for the 'Era' petascale supercomputer of Computer Network Information Center of Chinese Academy of Sciences is gratefully acknowledged.

REFERENCES

[1] Chris Baker. The flow around high speed trains[J]. Journal of Wind Engineering and Industrial Aerodynamics. 98, 277-298. 2010.

[2] Hassan Hemida, Sinisa Krajnovic. Numerical study of the unsteady flow structure around train-shaped body subjected to side winds[C]. European Congress on Computational Methods in Applied Sciences and Engineering (ECCOMAS). Netherlands, 2006.

[3] Zhigang Yang, Jing Ma, Yu Chen et al. The Unsteady Aerodynamic Characteristics of a High-speed Train in Different Operating Conditions under Cross Wind [J]. Journal of the China Railway Society. 32(2), 109-114. 2010, 4. (in Chinese)

[4] Chris Baker. The effect of unsteady crosswind forces on trains dynamic behavior[C]. EACWE 5, Florence, Italy. 2009, 7,19-23.

[5] C.J. Baker, J. Jones, F. Lopez-Calleja, et al. Measurements of the cross wind forces on trains[J]. Journal of Wind Engineering and Industrial Aerodynamics. 92, 547-563. 2004.

[6] Chris Baker, Federico Cheli, Alexander Orellano, et al. Cross-wind effect on road and rail vehicles[J]. Vehicle System Dynamics. 47 (8), 983-1019. 2009, 8.

[7] C. Baker, H. Hemida, S. Iwnicki, et al. Integration of crosswind forces into train dynamic modeling[J]. Proceedings of the Institution of Mechanical Engineers, Part F: Journal of Rail and Rapid Transit. 225, 154-164. 2010, 4.

[8] Sinisa Krajnovic, Hassan Hemida, Ben Diedrichs. Time-dependent simulations for the directional stability of high speed trains under the influence of cross winds or cruising inside tunnels[C]. Fluid Dynamics Appliction in Ground Transportation: Simulation, a primary development tool in the automotive industry. Lyon, France. 2005.

[9] Hassan Hemida, Sinisa Krajnovic, Lars Davidson. Large-eddy simulation of the flow around a simplified high speed train under the influence of a cross wind[C]. 17th AIAA Computational Fluid Dynamics Conference. Toronto, Ontario Canada. 2005, 6, 6-9.

[10] Sinisa Krajnovic, J. Georgii, Hassan Hemida. DES of the flow around a high speed train under the influence of wind gusts[C]. In: 7th International ERCOFTAC symposium on engineering turbulence. Modelling and measurements, ETMM7, 4 – 6 June, Amathus, Cyprus. 2008.

[11] Hassan Hemida, Sinisa Krajnovic. LES study of the influence of the nose shape and yaw angles on the flow structure around trains[J]. Journal of Wind Engineering and Industrial Aerodynamics. 98, 34-46. 2010.

[12] Hassan Hemida, Chris Baker. Large-eddy simulation of the flow around a freight wagon subjected to a crosswind[J]. Computer & Fluid. 39, 1944-1956. 2010.

[13] Ben Diedrichs, M. Sima, A. Orwllano, et al. Crosswind stability of a high-speed train on a high embankment[J]. Proceedings of the Institution of Mechanical Engineers, Part F: Journal of Rail and Rapid Transit. 221, 205-225. 2007.

[14] Ben Diedrichs. Aerodynamic calculations of crosswind stability of a high-speed train using control volume of arbitrary polyhedral shape[C]. BBAA VI International Colloquium on: Bluff Bodies Aerodynamics & Applications. Milano, Italy. 2008, 7, 20-24.

[15] W. Khier, M. Breuer, F. Durst. Flow structure around trains under side wind conditions: a numerical study[J]. Computer & Fluid. 29, 179-194. 2000.

[16] Dan Zhou, Hongqi Tian, Zhaijun Lu. Influence of strong crosswind on aerodynamic performance of passenger train running on embankment [J]. Journal of Traffic and Transportation Engineering, 7(4), 6-9. 2007, 8. (in Chinese)

[17] Dan Zhou, Hongqi Tian, Mingzhi Yang et al. Comparison of Aerodynamic Performance of Different Kinds of Wagons Running on Embankment of the Qinghai-Tibet Railway under Strong Crosswind [J]. Journal of the China Railway Society. 29(5), 32-35. 2007, 10. (in Chinese)

[18] Dan Zhou, Hongqi Tian, Mingzhi Yang et al. Comparison of aerodynamic performance of passenger train traveling on different railway conditions up strong cross-wind [J]. J. Cent. South Univ. (Science and Technology). 39(3), 554-559. 2008, 6. (in Chinese)

[19] Yiwei Wang, Yang Wang, Yiran An et al. Aerodynamic simulation of high-speed trains based on the Lattice Boltzmann Method [J]. Sci China Ser E-Tech Sci 51(6), 773-783. 2008.

[20] Jing Ma, Jie Zhang and Zhigang Yang, Study on the Unsteady Aerodynamic Characteristics of a High-speed Train Under Cross Wind [J]. Journal of the China Railway Society. 30(6), 109-114. 2008, 12. (in Chinese)

[21] Shur, M.L., Spalart, P.R., Strelets, M.K., Travin, A.K.: A hybrid RANS-LES approach with delayed-DES and wall-modeled LES capabilities. Int. J. Heat Fluid Flow 29, 1638–1649 (2008)

[22] Eiji Shima, Keiichi Kitamura, and Takanori Haga. "Green–Gauss/Weighted-Least-Squares Hybrid Gradient Reconstruction for Arbitrary Polyhedra Unstructured Grids", AIAA Journal, Vol. 51, No. 11 (2013), pp. 2740-2747.

[23] Jasak H., Weller H.G., and Gosman A.D. “High Resolution Differencing Scheme for Arbitrarily Unstructured Meshes”. International Journal for Numerical Methods in Fluids. Vol. 31. 431-449. 1999.

[24] Shuanbao Yao, Zhenxu Sun, Dilong Guo, et al, Numerical Study on Wake Characteristics of High-Speed Trains, Acta Mech. Sin., 29(6), 811–822, 2013.